Multitype Drone Mapping Technology Based on Refined Real-Scene 3D Modeling

Lingfeng Chen a, Zheng Ji a,*, Yang Lyu a, Anqi Du a, Xiangxiang Huang b

Abstract: With the rapid advancement of drone technology, its applications in the field of mapping have been continuously expanding in both scope and depth. Compared to traditional mapping techniques, drones have emerged as a critical tool for geographic information collection due to their efficiency, flexibility, and cost-effectiveness. This paper focuses on widely used flight path planning methods for drones in the context of mapping and proposes an object-oriented three-dimensional(3D) flight path planning method, which enables more intelligent and precise flight path planning by integrating the characteristics of object features. Additionally, the study explores mapping techniques based on refined 3D models, where the refined models are utilized to generate various types of mapping products. The findings of this research offer novel solutions and promising development prospects for the drone-based mapping industry, paving the way for smarter, more accurate, and diversified mapping applications.

Keywords: drone, path planning, drone mapping, refined 3D model

1. Introduction

In the 21st century, drone-based mapping technology has undergone significant breakthroughs. Advances in hardware have led to lighter drone designs, extended flight durations, and improved wind resistance. Simultaneously, aerial survey equipment has seen substantial performance enhancements, with integrated high-resolution, multispectral, and thermal imaging sensors enabling drones to capture richer and more detailed geographic information.

Over the past decade, improvements in drone mapping software and the increasing intelligence of flight control systems have enhanced drones' capabilities in autonomous planning and obstacle avoidance(Arafat et al., 2023). The integration of drones with emerging technologies such as cloud computing, big data, and the Internet of Things (IoT) has expanded their applications to complex projects, including urban 3D modeling and disaster response. By connecting to ground stations and data centers via networks, and leveraging deep learning and big data technologies, drones have significantly improved real-time data processing and information extraction.

Concurrently, policies governing drone mapping have been steadily refined. For instance, the FAA introduced the Small UAS Rule in 2016, and China enacted a series of drone management regulations starting in 2017.

From its origins in military applications, drone mapping technology has evolved into an efficient and intelligent tool widely employed across various civilian domains(Nex et al., 2022).

1.1 Historical background

The journey of drone-based mapping began with the aspiration to gain a bird's-eye view of the world. In the 1850s, French photographer Gaspard-Félix Tournachon demonstrated early attempts at aerial surveying using hot air balloons(Dunbar et al., 2023). While groundbreaking, these initial efforts were hampered by the unpredictable nature of balloons.

The advent of airplanes brought new possibilities for aerial photography, with Wilbur Wright capturing the first aerial photograph from an aircraft in 1909. The strategic significance of aerial mapping became evident during World War I, as reconnaissance aircraft equipped with cameras played a pivotal role in tracking enemy positions.

In 2013, Chinese drone manufacturer DJI released its first commercial drone equipped with a high-resolution camera, the Phantom 1, marking a significant leap in drone mapping technology(Rakha & Gorodetsky, 2018). This ready-to-fly system, equipped with a built-in GPS, offered stable and reliable flight experiences, making drone operation more accessible and safer. This innovation paved the way for the widespread adoption of drone-based photogrammetry, a technique for creating accurate maps and 3D models using photographs, establishing DJI as the first company to produce drones that were user-friendly for the general public. Building on this momentum, DJI continued to release a series of innovative drones, cementing its position as the world's leading drone manufacturer. Subsequent models, such as the Phantom 4 RTK and the Mavic 3 Enterprise series, have been widely adopted in the mapping industry.

^a School of Remote Sensing and Information Engineering, Wuhan University, whuchenlingfeng@whu.edu.cn, jz07@whu.edu.cn, lysunny2003@whu.edu.cn, 2020302131279@whu.edu.cn

^b School of Big Data and Artificial Intelligence, Chizhou University, xxh897@czu.edu.cn

^{*} Corresponding author

1.2 Difference between different mapping methods

The commonly used mapping technologies now primarily include satellite mapping and engineering mapping. Satellite mapping offers extensive coverage and long revisit cycles, with resolutions typically at sub-meter levels, making it suitable for large-scale geographic information acquisition projects. However, it is characterized by high costs and limited flexibility and real-time responsiveness. Traditional engineering mapping, on the other hand, relies heavily on the specific project requirements for accuracy and efficiency, necessitating professional survey teams and equipment, which also results in relatively high costs.

In contrast, drone mapping stands out with its numerous advantages, including high efficiency, high image resolution, low costs, minimal equipment wear and tear, low risks, and reusability. Drones can capture highresolution images below cloud cover, at low altitudes. Their ability to operate at moderate altitudes reduces the of obtaining complexity airspace permissions, significantly shortening task completion times. Drones are also highly maneuverable, easy to maintain and operate, and require lower levels of professional expertise from operators, making them an effective tool for obtaining high-scale imagery data over medium and small

Drones are particularly effective for a variety of tasks, including precision agriculture, powerline inspection, disaster emergency response, wildfire monitoring, heritage site monitoring, and mining area mapping(Mohsan et al., 2022). With drones, these tasks can often be completed with high efficiency and precision, highlighting their utility in diverse applications.

2. Drone mapping workflow and methods

2.1 Drone mapping workflow

The workflow for drone mapping, as illustrated in Figure 1, consists of five primary stages: preparation, flight path planning, data acquisition, data processing, and result output. Below is a detailed explanation of each phase.

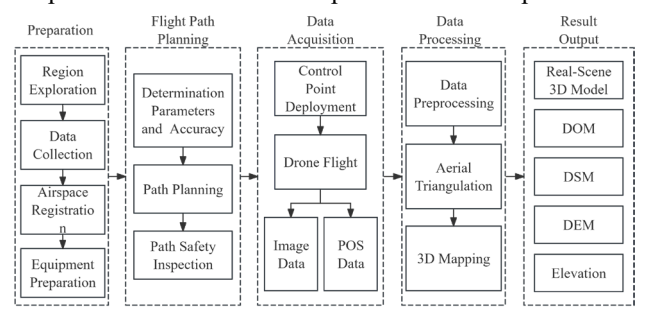


Figure 1. Workflow for drone mapping.

2.1.1 Preparation

Based on the mapping requirements, determine the area for mapping and collect existing topographic maps and control point coordinates within the area to provide references and accuracy validation for subsequent processing. Additionally, prepare and calibrate equipment, select drones equipped with appropriate sensors, and set up ground control point measurement equipment such as total stations and GPS receivers.

2.1.2 Flight path planning

When planning the flight path, considering the terrain and mapping precision requirements of the target area, select an appropriate flight path type, and determine suitable flight parameters. Ensure that the flight path covers the entire area and that the captured images have a certain degree of overlap. Additionally, perform safety checks on the flight path, considering terrain variations and obstacles to prevent drone collisions during flight.

2.1.3 Data acquisition

Carry out drone flights along the planned flight paths, ensuring stable flight and clear imagery. During the flight, observe the drone's flight status and image quality, and make adjustments as necessary if issues arise. After the flight, inspect the captured image data to evaluate whether the quantity, quality, and overlap of the images meet requirements, and conduct supplementary flights if necessary.

2.1.4 Data processing

Process the collected imagery through algorithms such as geometric correction, image stitching, and image enhancement to improve image quality. Automatically match feature points on the images, calculate the exterior orientation elements and coordinates of densification points, and establish a 3D coordinate system for the imagery. Based on aerial triangulation results, correct the image data to eliminate distortions and errors.

2.1.5 3D mapping and result output

To obtain effective information such as the 3D terrain of the target area, use the corrected image data for 3D mapping. The specific methods of 3D mapping may vary depending on the type of data source, including 3D model reconstruction, digital surface model generation, and digital elevation model generation. Finally, annotate the results of the 3D mapping, organize and check the topological relationships and attribute information for correctness, and identify any missing or misinterpreted data. Output the final 3D products that meet precision requirements, such as refined 3D models, digital line graphs, digital elevation models, and digital surface models.

2.2 Drone flight path planning methods

Common flight path planning methods as illustrated in Figure 2, can generally be divided into three categories: 2D planning, 2.5D planning, and 3D planning.

Among these, 2D flight path planning methods primarily includes traditional aerial photogrammetry, oblique photogrammetry, and circular path planning. In 2D planning, drones typically fly at a fixed altitude. And traditional aerial photogrammetry and circular path planning often adopt a vertically downward perspective, while oblique photogrammetry commonly uses five-directional cameras or cameras with specific oblique

angles. In terms of flight paths, traditional aerial photogrammetry and oblique photogrammetry mainly use regular grid-like patterns, whereas circular path planning relies on multiple overlapping circular paths to cover the target area. This method is suitable for relatively flat terrain, with flight altitude and path spacing or circular parameters determined based on 2D maps. Only the drone's position and flight altitude H need to be defined. However, when the terrain of the target area is significantly uneven, the images may exhibit notable geometric distortions and resolution differences, affecting reconstruction accuracy.

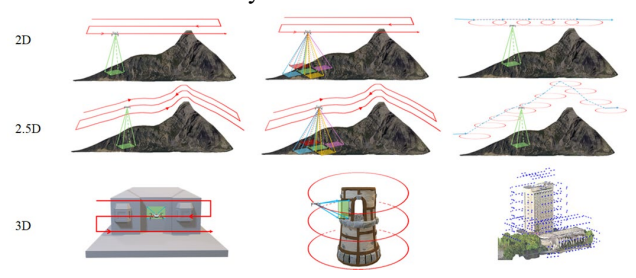


Figure 2. Common flight path planning methods.

2.5D flight path planning builds on 2D planning by introducing elevation information and adjusting the fixed flight altitude H to a variable altitude. This method typically uses a digital elevation model (DEM) as the initial reference, maintaining a consistent photography distance to some extent to mitigate inconsistencies in image resolution. However, since the camera angle remains fixed, image distortion issues still persist.

3D flight path planning differs significantly from the previous two approaches, with flight paths closely following the target surface and consistently oriented toward the surface. Most current 3D flight path planning methods rely on an initial 3D model of the target, which is used to calculate the drone's position and camera orientation. This initial 3D model is often generated using 2D flight path planning. The significant advantage of 3D planning is its ability to comprehensively and meticulously capture target information, particularly the sides of buildings. Furthermore, due to the high precision and flexibility required for flights close to the target surface, multi-rotor drones equipped with functionality are typically used. These drones can achieve photography distances as short as 5 meters or less, capturing millimeter-level images. Additionally, cameras equipped with gimbals ensure flexibility and control of the viewing angle.

2.3 3D flight path planning for complex scenarios

With the continuous advancement of drone technology, there is a growing demand for more refined flight path planning and data collection. In fields such as urban planning, autonomous driving, and archaeological studies, generating refined 3D models is of critical importance. Traditional drone mapping methods with 2D and 2.5D flight path are increasingly unable to meet the requirements for refined data acquisition in complex

scenarios, necessitating the development of more advanced and refined 3D flight path planning methods.

As illustrated in Figure 3, 3D flight path planning involves two key components: geometric analysis of photographic objects and safety analysis of the spatial environment(Zhou et al., 2023). First, based on the initial model that includes spatial constraints and coordinate information for photographic objects, flight requirements and reconstruction constraints such as sensor parameters, image resolution, intersection angles, and overlap are taken into account. For the selected surface objects, the normal vectors are extracted to determine the drone's photography orientation, serving as spatial geometric constraints for the objects. By integrating these factors, photographic viewpoints corresponding to the objects are generated, thus completing the generation of viewpoints for the entire scene.

Second, when dealing with complex spatial scenarios, flight path planning for drones requires a thorough safety of the spatial environment. Obstacles encountered during flight can impose spatial restrictions on drone pathways, necessitating the rational planning of no-fly zones to ensure safe operations. Additionally, the limitations of the drone itself must be considered, such as the minimum flight distance, battery endurance, and the effects of environmental factors like weather on flight stability and positioning. By comprehensively addressing these constraints and requirements, drones can perform close-range flights over target scenes, capturing complete high-resolution images. This approach reduces data redundancy while producing high-quality, detailed, and realistic 3D models.





(a) target areas

(b) photographic viewpoints.

Figure 3. Drone 3D flight path planned based on the initial model. The green boxes represent target areas, red areas denote no-fly zones, blue points indicate photographic viewpoints.

3. Object-oriented 3d drone path planning

In current commonly used flight path planning software, objects selection is typically performed manually. This makes it challenging to handle irregularly shaped or rotated target objects and increases both operational complexity and the learning curve. Furthermore, some existing flight path planning algorithms based on initial models generally analyze the surface of 3D mesh models to generate sampling points, which serve as the foundation for viewpoint selection and path planning. Nevertheless, the sampling points generated by these algorithms are often weakly correlated with the geometric characteristics of the objects, and the distribution of photography points tends to be disorganized, making it difficult to meet the precision requirements of drone

flight control. Therefore, we have adopted an objectoriented 3D flight path planning strategy.

3.1 The target objects for flight path planning.

The object-oriented flight path planning method requires a clear definition of the planning objectives prior to design. Based on the characteristics of object-oriented photogrammetry, this paper defines four foundational geometric objects for aerial photography: points, lines, surfaces, and prisms, as illustrated in Figure 4. These are used for objects selection. During the selection process, the target surface can be segmented and combined based on these geometric objects to identify surface points, which are then discretized into photography points. Surface normal vectors are utilized to determine the photography direction. Any target entity can be represented through these four geometric objects or their combinations, enabling comprehensive objects selection and coverage in the 3D space. The definitions and applicable scenarios of these four foundational geometric objects will be detailed as follows.

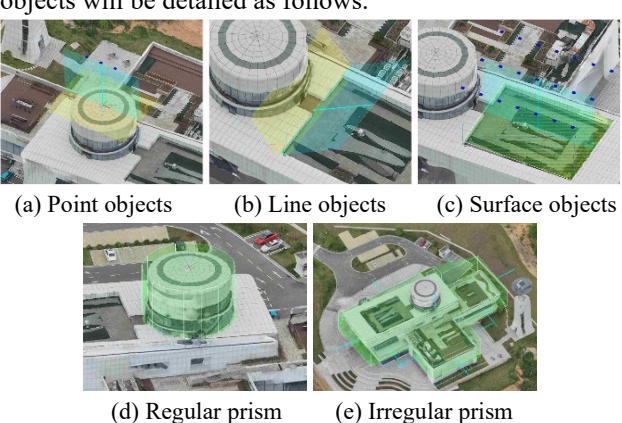


Figure 4. Examples of the four foundational geometric objects.

Point objects represent the simplest type of geometric objects. For a single point on the target surface, the corresponding photography point and direction can be determined based on its position and the local surface normal vector. Point objects are typically used for tasks such as retaking specific locations or addressing scattered tasks in special areas.

Line objects are defined by two points on the target surface. The initial photography direction is determined by averaging and normalizing the surface normal vectors of these two points. Line objects are primarily used for handling discontinuous boundary regions of target entities. For special areas, the appropriate photography direction can be determined by adjusting the two degrees of freedom associated with yaw and pitch angles.

Surface objects refer to planar areas within a certain range on the target surface. Their photography direction can be directly determined by the surface normal vector. Surface objects are mainly applied to large, flat regions. Accurate representation of the surface normal vector requires computational determination to ensure precise depiction of the surface.

Prism objects are represented as 3D polyhedra, which can be classified into regular and irregular prisms. A regular prism object has a base that is a regular polygon with uniform side heights, while an irregular prism object has a base that is an irregular polygon. The photography task for the prism objects is accomplished by generating photography surfaces on the faces of prism. The surfaces of the prism constitute the photography object surfaces, which mathematically represent a combination of multiple contiguous surface objects. The photography direction of each surface object is parallel to its surface normal vector.

3.2 Automatic surface objects extraction based on planar segmentation

In the task of selecting photogrammetric objects, surface objects are often used to represent extensive target surfaces to be reconstructed. These objects possess relatively stable geometric characteristics, making them the most commonly utilized among the four foundational geometric objects in drone 3D flight path mapping. Consequently, designing an automatic extraction process for surface objects in the initial model can significantly reduce manual selection efforts and enhance the efficiency of the objects selection phase.

The method proposed in this study involves operations such as mesh segmentation, plane fitting, and polygon extraction on the triangular mesh model of the target surface. This process generates surface objects suitable for subsequent photogrammetric design tasks.

3.2.1 Region-Growing-based planar segmentation

The region growing algorithm is one of the commonly used methods for mesh segmentation. This type of method begins by selecting a seed from a subset of patch sets within a 3D mesh. Subsequently, based on predefined judgment criteria, other elements that meet the conditions are gradually merged into the existing cluster, forming a sub-mesh. Mesh attributes are commonly employed in the segmentation and processing of meshes to determine division conditions. These attributes include various forms such as planarity, angular distance between patches, concavity/convexity, curvature, and geodesic distance.

We employ a region growing algorithm based on the kring neighborhood planarity of mesh vertices to segment and extract planar regions from 3D mesh models of reconstruction objects(Bouzas et al., 2020). For a vertex in a mesh, its 1-ring neighborhood is defined as the set of all vertices directly connected to it via edges, while its 2-ring neighborhood additionally includes vertices adjacent to those in the 1-ring neighborhood. By analogy, the concept of a k-ring neighborhood for mesh vertices can be derived. The planarity of a vertex's k-ring neighborhood represents the degree of planar fitting in that neighborhood, and the planarity of a face is defined as the average planarity of its vertices. The algorithm proceeds as follows:

1) Compute the planarity of the k-ring neighborhood for all vertices in the 3D mesh. Use the average planarity

- of the vertices within each face to represent the planarity of that face.
- 2) Choose the face with the highest planarity as the seed. Use its k-ring neighborhood as the initial planar region and determine the reference plane using Principal Component Analysis (PCA).
- Examine the k-ring neighborhood of the seed, merging faces whose vertices are within a predefined distance threshold from the reference plane into the current planar region.
- 4) Repeat the above process until the entire 3D mesh is decomposed into distinct planar regions, completing the segmentation and yielding the segmentation results for each planar region.

The key parameters in this mesh segmentation process are neighborhood range and distance threshold. A smaller neighborhood range makes the segmentation less sensitive, while a larger range significantly increases the computational time for planarity calculations and patch merging. In this study, neighborhood range was set to 3. Distance threshold must be set based on the scale of the initial mesh model. In this study, the average edge length of the initial mesh model was used as the distance threshold. This approach enhances the adaptability of the merging criteria to diverse datasets.

3.2.2 Surface objects extraction

To obtain the surface objects required for flight path planning, it is necessary to extract polygons representing surface objects from the results of mesh segmentation. The mesh segmentation step results in subsets of meshes belonging to the same planar region, along with their corresponding fitted plane equations. By projecting the vertices within the segmented mesh subsets onto the fitted plane, the problem of extracting polygons from the 3D mesh is transformed into a 2D plane problem which essentially involves determining the boundary contour of the region occupied by the point set and reconstructing a reasonable geometric shape. For the surface target extraction steps in this study, the possibility of concave shapes must be considered, necessitating the use of concave hulls for point set boundary extraction. The Alpha-shape algorithm is an effective method for extracting boundary contours points(Edelsbrunner et al., 1983). The basic idea of the algorithm is as follows: given a circle with a radius of r, the circle rolls around the point set, and by selecting an appropriately sized parameter α , the points that the circle passes through are connected to form the boundary of the point set.

To further elaborate on this concept, the algorithm extends the convex hull by introducing a parameter α , which imposes a length constraint on the edges of the extracted contour polygon. This makes the boundary extraction result different from the convex hull result, as it avoids connecting points that are too far apart. When the value of parameter α approaches infinity, the extracted boundary result converges to the convex hull. Conversely, when the parameter α is smaller and results

are extractable, the algorithm can generate a point set boundary with concavities, effectively representing the shape of the point set.

Based on the concept of the Alpha-shape algorithm, we extract boundary contours for coplanar point sets obtained from the projected results of mesh segmentation.

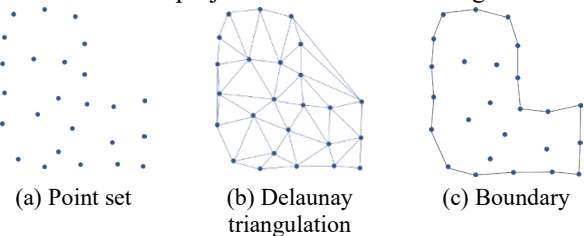


Figure 5. Illustration of the boundary extraction Process.

The schematic diagram of polygon extraction using this method is shown in Figure 5, with the specific steps as follows:

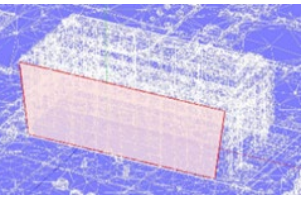
- 1) Construct a Delaunay triangulation for the input coplanar point set.
- Compute the lengths of all edges in the triangulation and their adjacent triangle sets, defining edges with only one adjacent triangle as the boundary edges of the point set.
- 3) Add all boundary edges with lengths greater than the threshold to queue. For an edge in queue, remove it from the adjacency triangle sets of the two other edges in its unique adjacent triangle, and add the edges longer than the threshold to queue. Repeat this step until the queue is empty.
- Output all remaining boundary edges shorter than the threshold to represent the boundary shape of the point set.

The boundary contour lines extracted from the vertex data of mesh subsets are typically very rough and even jagged, which increases data storage burdens and hinders subsequent flight path generation. Therefore, after obtaining the original boundary contour lines, it is necessary to simplify them to generate skeleton lines of the contours. We use the Douglas-Peucker algorithm to reduce the points of the original contour lines, generating the final polygons representing surface targets.

The method first connects the start and end points of the boundary edge set with a straight line, calculates the maximum distance from all intermediate points to the line, and if this maximum distance is smaller than a predefined threshold, only these two points are retained for this segment, completing the process. Otherwise, the point corresponding to the maximum distance is taken as an intermediate point, dividing the contour line into two segments. The above steps are repeated for each segment until all contour segments are processed, and the divided points are sequentially connected to form the simplified polygonal contour line.

The extracted surface object results are shown in Figure 6. As shown in Figure 6(b), the red polygon is one of the extracted surface objects of the building.





(a) Objects in solid view

(b) Objects in wireframe view

Figure 6. Example of surface objects extraction. The red polygon is one of the extracted surface objects of the building.

3.3 Path generation based on extracted objects

After identifying the objects to be reconstructed, photography design is performed in flight path planning based on its surface information. We introduce the concepts of target surface structural lines and basic flight strip units based on the principles of conventional aerial photogrammetry.

Structural lines are used to describe the geometric shape of the target surface, primarily in the horizontal direction. The target instances corresponding to the four basic aerial photography geometric objects defined earlier can essentially be transformed into structural lines or their combinations.

Considering the accuracy requirements of reconstruction, factors such as overlap, photographic distances and intersection angles are determined to sample and generate structural lines for the surface objects. Each structural line corresponds to a normal vector. For each individual structural line, discrete points are generated. The photography points generated by a single structural line ultimately form the basic flight strip unit for drone path.





(a) frontal

(b) cross-directional

Figure 7. Examples of frontal photography and cross-directional photography.

In addition to object-oriented frontal photography, the accuracy and completeness of refined reconstruction results can be ensured by increasing the intersection angles between stereo image pairs, achieving cross-directional photography from four angles (up, down, left, and right) of the target surface. When generating cross-directional photography waypoints, the yaw or pitch angle of the gimbal can be adjusted by increasing or decreasing an angle. Figure 7 illustrates the comparison between frontal photography and the addition of left and right cross-directional photography.

For the problem of path searching to connect basic flight strip units, this we use a graph data structure to construct a heterogeneous traveling salesman problem (TSP), where the basic flight strip units serve as nodes in the graph, and the goal is to find the minimum-cost connecting path between nodes. The cost between any two nodes is defined from the perspective of drone energy consumption, considering the horizontal and

vertical distances as well as the required changes in flight angles between the two nodes. The constructed cost function is shown in Equation (1):

$$\Delta \tau = \alpha \cdot \Delta XY + \beta \cdot \Delta Z + \gamma \cdot \varphi \tag{1}$$

Where ΔXY is the horizontal distance between two connected points on flight paths and ΔZ is the vertical distance between two connected points on flight paths and ϕ represents the turning angle between the two nodes, and α , β , γ represent the weights of the three reference factors.

To ensure the safety of the final flight path, the RRT* algorithm is used to determine a collision-free connection route between two nodes when obstacles are encountered during the connections between nodes(Karaman & Frazzoli, 2011).

3.4 Experiment

To verify the effectiveness of the proposed method, we compared our approach with oblique photogrammetry. Using images collected along the flight paths for 3D reconstruction, the resulting model is shown in Figure 8. From the figure, it is evident that the model generated by our method is more refined and complete, particularly in the depiction of building façades.





(a) Oblique photogrammetry

(b) Proposed method

Figure 8. Comparison between proposed method and oblique photogrammetry.

4. Multi-Type Mapping Products Based on Refined Real-Scene 3D Models

These refined real-scene 3D models, obtained through object-oriented flight path planning, featuring precise coordinate data and realistic texture information, enable comprehensive reproduction of the terrain and topography of target areas. Various mapping products can be generated by rendering virtual imagery based on these refined 3D models which can provide reliable data support for many fields, including urban planning, environmental monitoring, and heritage conservation.

4.1 Virtual imagery rendering method

To create virtual images from these mesh models, various available renderers can be employed. In this study, we utilized the OpenGL renderer. OpenGL, maintained by the Khronos Group, is a collection of graphics rendering API specifications. Its functionality is implemented by graphics card manufacturers based on these specifications. This approach ensures flexibility and efficiency in

generating virtual images while leveraging existing rendering technologies for high-quality outputs.

The imaging principle of OpenGL involves transforming input 3D vertex data, combined with texture information and various rendering states, into two-dimensional pixel fragments displayed on the screen. By integrating the mechanisms of photogrammetry, this process introduces the geometric transformations and imaging steps involved in virtual rendering. In the context of real-world 3D models, OpenGL determines the parameters of the virtual camera based on the principles of perspective projection or orthographic projection and subsequently renders lighting and texture to generate new images.

the After obtaining imaging parameters photogrammetry, specifically the camera pose, these parameters are used as the new imaging viewpoint for the model. This enables the transformation of 3D model points within the projection range corresponding to this viewpoint into 2D screen images. The process involves applying composite transformations, such as rotation, translation, and scaling, to the real-world 3D model points. Once transformed into the image space coordinate system, only objects within the view frustum can be captured by the camera. These points are subsequently converted to clip space using the perspective projection matrix. Through homogeneous division, they are then transformed into normalized device coordinates (NDC) and finally mapped to screen image coordinates. The transformation equations are provided in Equation (2)(Liu et al., 2023).

$$\begin{bmatrix} x & y & 1 \end{bmatrix}^{T} = F \cdot P \cdot M \cdot \begin{bmatrix} X & Y & Z & 1 \end{bmatrix}^{T}$$
$$F \cdot P \cdot M \sim \{R, c\}$$
 (2)

Where $[x \ y \ 1]^T$ represents the observed image coordinates, $[X \ Y \ Z \ 1]^T$ denotes the 3D model coordinates, and $F \cdot P \cdot M$ corresponds to the affine matrix, projection matrix, and model transformation matrix, respectively.

In addition, to accelerate computations, we employed depth buffering technology (Z-buffer), which is a crucial technique in computer graphics for addressing visibility issues in 3D scenes. During the process of generating virtual photographs in computer graphics, the depth buffer acts as a "distance memory." The system allocates a storage space for the depth value of each pixel on the display screen to record the distance between the object's surface at that position and the camera. Before rendering begins, the system initializes the depth values of all pixels to the maximum possible distance (commonly represented as 1.0). During rendering, when the system attempts to draw a new object surface at a specific pixel position, it first calculates the distance of the surface to the camera (the depth value) and then compares it with the current depth value stored at that pixel. This comparison follows a simple rule: if the depth value of the new object surface is smaller (i.e., closer to the camera), the system updates the depth value for that pixel and renders the new surface in the color buffer. Conversely, if the depth value of the new surface is larger (i.e., farther from the camera), the original depth value

remains unchanged, and the new surface is not rendered. Through this precise depth comparison mechanism, the depth buffer effectively ensures that objects in a 3D scene are displayed according to their correct spatial relationships, thereby generating virtual images that adhere to visual principles.

By integrating the model's vertex data, including position coordinates, texture coordinates, normal vectors, and colour, these attributes are transformed into fully rendered pixels to generate virtual observation images corresponding to a specified camera pose. As illustrated in Figure 9, the image in 9(a) represents the original capture obtained from the drone, while the image in 9(b) corresponds to the virtual observation image generated through rendering.



(a) Original image

(b) Rendering image

Figure 9. The results of rendering.

4.2 Mapping products

By leveraging refined real-scene 3D models and virtual image rendering technologies, a wide range of mapping products can be generated according to specific requirements. By projecting the refined 3D model onto the XY plane, a DOM can be generated, as shown in Figure 10. Furthermore, cross-sectional views from arbitrary perspectives can be produced. Compared to traditional orthophoto generation methods, crosssectional rendering based on refined 3D models offers superior flexibility and image quality, making it highly applicable in fields such as cultural heritage preservation, building inspections, and disaster monitoring. Besides, utilizing the parameters of drone cameras, virtual drone images can be generated from any desired location. By comparing time-series images captured by drones with virtual images rendered from the refined 3D models, effective change detection and analysis can be performed. As shown in Figure 11, by rendering the refined reconstruction results of the Xuankong Temple in Shanxi, an elevation view is generated, and a line drawing is produced(He, 2019). This method effectively captures the

intricate details of the ancient architecture, providing

valuable support for cultural heritage preservation.



(a) Refined 3D Model

(b) DOM

Figure 10. Refined 3D Model and DOM.



Figure 11. Elevation and line drawing of Xuankong Temple.

In the past, geological disaster investigations often relied on manual methods, which were both arduous and hazardous. However, through the generated elevation views from the refined 3D models, investigators can directly identify and interpret geological features, such as cracks and other potential risk information. Figure 12 shows the elevation view of the hazardous rock at Jianchuandong along the Yangtze River, generated from a refined 3D model. Through analysis of the elevation, cracks and other dangerous factors can be clearly

identified, greatly improving the efficiency and accuracy

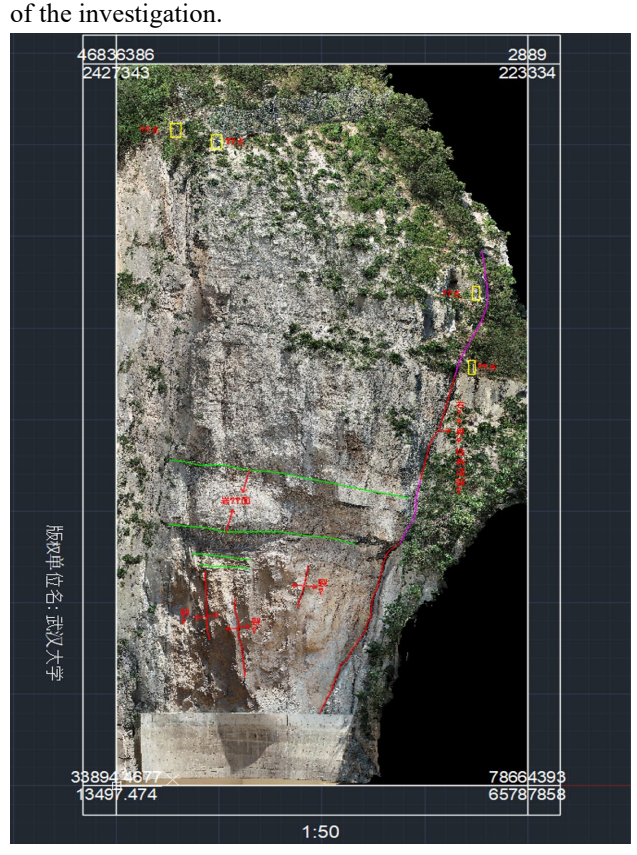


Figure 12. Elevation view of Jianchuandong generated from refined 3D models.

5. Conclusion

We systematically analyzed the development of drone mapping technology and common drone mapping methods, proposing an object-oriented 3D flight path planning method to efficiently acquire refined real-scene 3D models while ensuring safety. This method leverages plane segmentation and surface objects extraction techniques to generate object-oriented flight path plans, enabling drones to capture target images in closer and

more flexible ways, thereby facilitating the construction of refined 3D models. Furthermore, the study employs a virtual image rendering method based on OpenGL to visually present drone mapping results. The findings of this research provide significant technical references and support for the theoretical development and practical application of drone mapping technology.

6. Acknowledgements

Funded By Open Research Fund Program of LIESMARS, 23E04.

7. References

Arafat, M. Y., Alam, M. M., & Moh, S. (2023). Vision-Based Navigation Techniques for Unmanned Aerial Vehicles: Review and Challenges. Drones, 7(2), Article 2.

Bouzas, V., Ledoux, H., & Nan, L. (2020). Structure-aware Building Mesh Polygonization. ISPRS Journal of Photogrammetry and Remote Sensing, 167, 432–442.

Dunbar, M. B., Caballero, I., Román, A., & Navarro, G. (2023). Remote Sensing: Satellite and RPAS (Remotely Piloted Aircraft System). In J. Blasco & A. Tovar-Sánchez (Eds.), Marine Analytical Chemistry (pp. 389–417). Springer International Publishing.

Edelsbrunner, H., Kirkpatrick, D., & Seidel, R. (1983). On the shape of a set of points in the plane. IEEE Transactions on Information Theory, 29(4), 551–559. IEEE Transactions on Information Theory.

He, J. (2019). Nap-of-the-Object Photogrammetry and Its Key Techniques [Doctoral dissertation]. Wuhan university.

Karaman, S., & Frazzoli, E. (2011). Sampling-based Algorithms for Optimal Motion Planning (No. arXiv:1105.1186). arXiv.

Liu, Y., Ji, Z., Chen, L., & Liu, Y. (2023). Linear target change detection from a single image based on three-dimensional real scene. The Photogrammetric Record, 38(184), 617–635.

Mohsan, S. A. H., Khan, M. A., Noor, F., Ullah, I., & Alsharif, M. H. (2022). Towards the Unmanned Aerial Vehicles (UAVs): A Comprehensive Review. Drones, 6(6), Article 6.

Nex, F., Armenakis, C., Cramer, M., Cucci, D. A., Gerke, M., Honkavaara, E., Kukko, A., Persello, C., & Skaloud, J. (2022). UAV in the advent of the twenties: Where we stand and what is next. ISPRS Journal of Photogrammetry and Remote Sensing, 184, 215–242.

Rakha, T., & Gorodetsky, A. (2018). Review of Unmanned Aerial System (UAS) applications in the built environment: Towards automated building inspection procedures using drones. Automation in Construction, 93, 252–264.

Zhou, H., Ji, Z., You, X., Liu, Y., Chen, L., Zhao, K., Lin, S., & Huang, X. (2023). Geometric Primitive-Guided UAV Path Planning for High-Quality Image-Based Reconstruction. Remote Sensing, 15(10), Article 10.